CHIN. PHYS. LETT. Vol. 36, No. 6 (2019) 066301

Negative Thermal Expansion of $GaFe(CN)_6$ and Effect of Na Insertion by First-Principles Calculations *

Meng Li(李蒙), Yuan Li(李媛), Chun-Yan Wang(王春艳), Qiang Sun(孙强)**

International Laboratory for Quantum Functional Materials of Henan, School of Physics and Engineering, Zhengzhou University, Zhengzhou 450001

(Received 4 March 2019)

We study the negative thermal expansion (NTE) properties and effect of Na insertion on the NTE of the framework material $GaFe(CN)_6$ by first-principles calculations based on density functional theory within the quasi-harmonic approximation. The calculated results show that the material exhibits NTE due to the low transverse vibrational modes of the CN groups. The modes demonstrate larger negative values of the mode Grüneisen parameters. Once Na is introduced in the framework of the material, it prefers to locate at the center of the quadrates of the framework material and binds to the four N anions nearby. As a consequence, the transverse vibrational mode of the CN group is clearly hindered and the NTE of the material is weakened. Our theoretical calculations have clarified the mechanisms of NTE and the effect of the guest Na on the NTE of the framework material.

PACS: 63.20.dk, 63.20.−e, 65.40.De, 65.40.−b DOI: 10.1088/0256-307X/36/6/066301

Most solids in nature expand on heating, but a few exhibit negative thermal expansion (NTE) due to their low-frequency phonons,[1−6] magnetic/electronic transitions[6−10] or size effect.[11,12] The NTE materials offer a promising possibility to tailor the coefficient of thermal expansion of materials to near zero so that they can be used in precise instruments, where low or zero thermal expansion is critical.

The NTE materials, where NTE is driven by low-frequency phonons, include flexible open framework oxides,[13−16] fluorides,[17−19] cyanides,[20−26] MOFs,[27−29] etc., among which the most typical are ZrW_2O_8 and ScF_3.[1,17,19] ZrW_2O_8 has been intensively studied and simple rigid unit modes (RUMs) are suggested to explain the origin of NTE in the oxides. However, molecular dynamics simulations demonstrated that a more flexible model should be adopted to explain the lattice dynamics behavior and the related NTE phenomenon. For ScF_3, a recent study revealed that the transverse vibrations of fluorine atoms play a critical role in its NTE.[19]

As a kind of cyanide-bridged system, Prussian blue analogues (PBAs) have attracted much attention in recent years due to their intriguing physical and chemical properties such as magnetism,[30] energy storage,[31] environmental catalysis[32] and drug delivering.[33] The PBAs have a unique flexible structure with linkages of –M–C≡N–M– (M=metals) consisting of an open framework structure, where NTE properties have been widely discovered in $LnCo(CN)_6$ (Ln=La, Pr, Sm, Ho, Lu, Y),[24] $M^{II}Pt^{IV}(CN)_6$ (M=Mn, Fe, Co, Ni, Cu, Zn, Cd),[21,23] and $YFe(CN)_6$.[26] As a member of the NTE open-framework materials, the family of PBAs is a good candidate for exploring new NTE materials and understanding the complicated NTE mechanism. Recently, interesting isotropic NTE has been experimentally found in the cubic $GaFe(CN)_6$ of PBAs over a wide temperature range.[34] It was also found that through insertion of guest Na/H_2O the thermal expansion of the material may be effectively turned from negative to positive.[35] In this Letter, we investigate the NTE properties and the effect of guest Na on the NTE of the material by first-principles calculations. Our results show that the material exhibits NTE mainly due to the low transverse vibrational modes of the CN group. The inserted Na prefers to locate at a position near the center of the quadrates of the channels and prohibit transverse oscillation of the CN group. Our theoretical calculations clarify the mechanisms of NTE and the effect of inserted Na on the NTE property of the framework material.

All our calculations are carried out using the first-principles method based on density functional theory as implemented in the Vienna *ab initio* simulation package (VASP).[36] The ion–electron interaction is depicted by the projector augmented wave (PAW) method,[37] and the exchange and correlation effects are described by the GGA-PBE functional.[38] The wave functions are expanded by the plane waves up to an energy cutoff of 520 eV. Integrals over the first Brillouin zone are approximated by a $9\times9\times9$ Monkhorst–Pack k-point mesh. The total energy is calculated with high precision, converged to 10^{-8} eV/atom, and the structural relaxation will be stopped when the residual forces become less than 10^{-4} eV/Å.

Vibrational properties are carried out using the supercell method and post-processed by the PHONOPY code.[39] The real-space force constants are calculated using the density-functional perturbation theory as implemented in the VASP code. Based on quasi-harmonic approximation (QHA), the thermal properties of the system are simulated. In QHA, the volume dependence of phonon frequencies at finite tem-

*Supported by the National Natural Science Foundation of China under Grant Nos 11874328 and 11372283.
**Corresponding author. Email: qsun@zzu.edu.cn
© 2019 Chinese Physical Society and IOP Publishing Ltd

perature is introduced as a part of the anharmonic effect.[40] When the temperature is away from the melting point, the QHA has been proved to be a good approximation. In our previous works,[41–44] this method was a significant success. Within the QHA, the Helmholtz free energy $F(V,T)$ has been calculated by[43,45]

$$F(V,T) = E_0(V) + F_{\rm vib}(V,T), \tag{1}$$

where $E_0(V)$ is the 0 K total energy of the solid at volume V, $F_{\rm vib}$ stands for the vibration energy given by

$$F_{\rm vib}(V,T) = k_{\rm B}T \sum_{v,\boldsymbol{q}} \log\left\{2\sinh\left(\frac{\hbar\omega_v(\boldsymbol{q},V)}{2k_{\rm B}T}\right)\right\}, \tag{2}$$

where $\omega_v(\boldsymbol{q},V)$ is the phonon frequency of phonon mode v with wave vector $\boldsymbol{q}$ of the solid at volume V. To obtain the influence of temperature on the volume, ten different volumes are selected near the optimized equilibrium position. At each volume point, internal atomic positions are optimized and the phonon dispersion curves are simulated using the method and parameters mentioned above. With the help of the Murnaghan equation of state, the isothermal F–V curves are fitted to harvest the Helmholtz free energies, which are obtained as the minimum values of the thermodynamic functions.

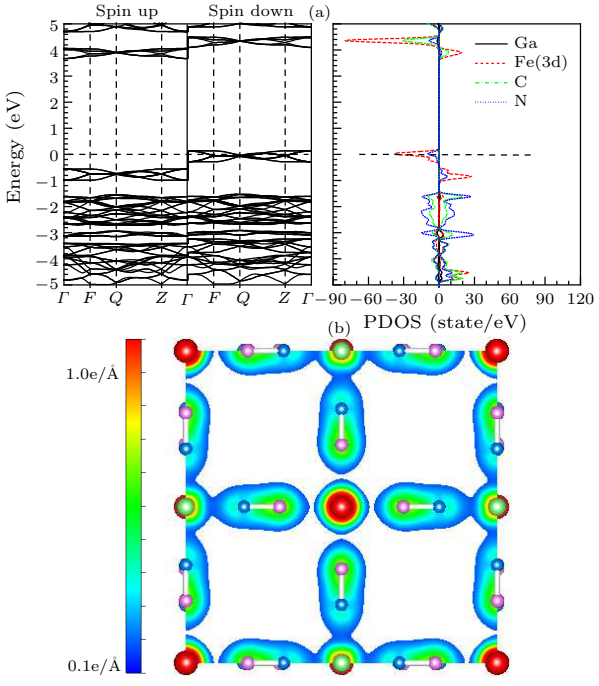

Fig. 1. (a) Electron band structure and PDOS of $GaFe(CN)_6$. (b) The total charge density of $GaFe(CN)_6$ in (001) plane.

$GaFe(CN)_6$ has a simple cubic symmetry, consisting of GaN_6 and FeC_6 of octahedron, which are connected by Fe–CN–Ga. The calculated structural parameters are: lattice constant $a = 10.19$ Å, bond length $d = 1.17$ Å (C–N), $d = 2.03$ Å (Ga–N), $d = 1.90$ Å (Fe–C), respectively, which are slightly larger than the experimental data[34] because we use the generalized gradient approximation (GGA) in the calculation.

The calculated electron partial density of states (PDOS) and band structure along the high symmetry direction in the first Brillouin zone are shown in Fig. 1(a), and the valence charge density distribution in plane (001) is given in Fig. 1(b). It can be clearly seen from the electronic structures that the electronic states of Fe and C are more overlapped than those of Ga and N, which indicates that the bond formed between Fe and C atoms is somewhat covalent and is stronger than that of the latter. Thus N atoms in the framework should be more flexible and easy to oscillate at a finite temperature, which is verified by the phonon density of states shown below. It can also be seen that the density of states of Fe 3d is spin-asymmetric near the Fermi level with a local magnetic moment of $1.0\mu_{\rm B}$ for Fe, indicating that $GaFe(CN)_6$ should demonstrate paramagnetic property [the distance of Fe–Fe is far away (distance 10.20 Å) and their magnetic coupling should be negligible]. Thus here only the phonon contribution to thermal expansion is considered due to the negligible magnetic coupling. Furthermore, the local magnetic moment of Fe can be destroyed by the insertion of Na.

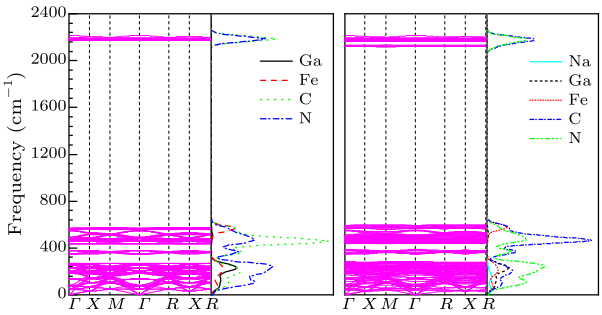

Fig. 2. (a) Phonon dispersion and phonon PDOS for the system $GaFe(CN)_6$. (b) Phonon dispersion and phonon PDOS for the system of one Na inserted $GaFe(CN)_6$.

The calculated phonon dispersion and phonon partial density of states (PDOS) of the system with and without Na insertion are given in Fig. 2. From the phonon dispersion shown in Fig. 2(a), the main four bands can be seen for the framework system: three low-frequency bands (0–300 cm^{-1}, 349–400 cm^{-1} and 420–580 cm^{-1}) and one high-frequency band (2041–2437 cm^{-1}). From the phonon PDOS, it can be seen that the transverse vibration of C contributes mostly to the lowest frequency band. Ga and Fe also contribute to the band. For the band 349–400 cm^{-1}, the contribution is from the transverse vibration of N and C in the opposite directions, while for the highest band, it originates from the stretch oscillation between C and N. These phonon band features can be explained by the symmetry and bond nature of the system. It can be seen in the following that the vibration modes in the lowest two bands have the largest contribution to the negative thermal expansion of the

system.

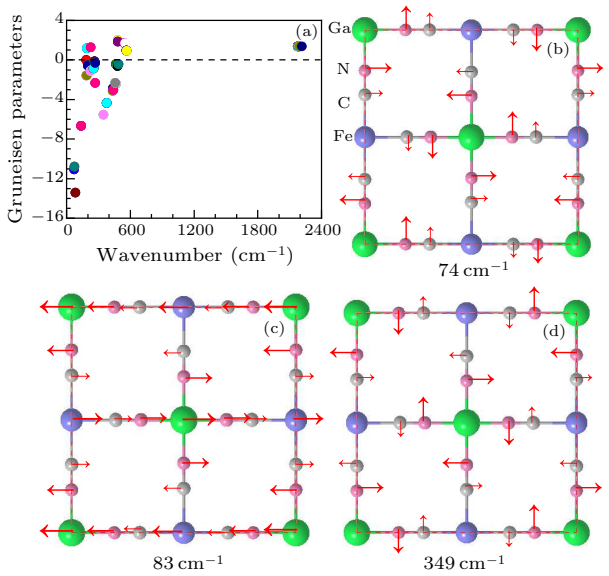

Fig. 3. (a) Calculated Grüneisen parameters of $GaFe(CN)_6$. (b), (c) and (d) The lowest vibration modes at the locations of 74 cm^{-1}, 83 cm^{-1} and 349 cm^{-1}, respectively, which have large negative Grüneisen parameters. Arrows indicate the vibrational directions of atoms.

To determine which phonon mode contributes mostly to the NTE property of the system, we calculate the mode Grüneisen parameters (modes at the Γ point) of the system as shown in Fig. 3(a). According to the relationship between the Grüneisen parameter and the volume coefficient of thermal expansion (CTE), we know that the phonon modes with negative Grüneisen parameter contribute to the NTE of the system. Our results reveal that the vibration modes in the low-frequency bands contribute mostly to the NTE of the system, and the three modes at 74 cm^{-1}, 83 cm^{-1} and 349 cm^{-1} with the large negative Grüneisen parameters (-11, -13 and -6, respectively) are shown in Figs. 3(b)–3(d), where the arrows indicate the directions of vibration. The mode in Fig. 3(b) shows that C and N move laterally in the same direction, and Ga and Fe atoms barely move, while in Fig. 3(c), the mode shows the transverse vibration of C and N in the opposite direction with Fe and Ga moving together with them, respectively. The mode with higher frequency (Fig. 3(d)) shows the transverse vibration of C and N in the opposite directions without Fe and Ga moving with them. In the highest frequency region, which originates from the CN stretch vibration, the Grüneisen parameters are positive, and they contribute to the positive expansion of the system. In brief, the NTE of the system is caused by the vibration of the low-frequency phonon modes where C and N move along the transverse direction (in the same or opposite direction) with N more flexible than C. These lateral vibrations make the distance between Fe and Ga shorter and the system exhibits NTE. Many NTE materials with framework structure own such vibration modes and their NTE mainly originates from the modes.[41,42]

The volume CTE of the system $GaFe(CN)_6$ is calculated in the temperature range 0–300 K as shown in Fig. 4(a). From the calculated results it can be seen that the calculated volume CTE is about -40×10^{-6} K^{-1}, which is lower than the experimental one $\sim -12 \times 10^{-6}$ K^{-1} (100–475 K).[34] The difference between the theoretical result and the experimental one may be attributed to the GGA and QHA.

Then one guest Na is introduced in the framework of the material and its effect on the NTE of the material is investigated. The first considered question is where the stable binding site is located for the inserted Na atom. The experimental observation shows that the guest Na seems to appear in the center of the small cubic structural unit (there are eight small cubic structural units in one cubic crystal unit cell) at room temperature.[35] However, after we put it at the position as the initial configuration for structural optimization, we find that the inserted Na finally approaches the center of the quadrate of the framework material and binds to four N anions nearby. Moreover, the existence of Na has a certain effect on the crystal structure: the angle of Ga–N–C is reduced to 175° (180° for the pristine system) after insertion of Na, and the distance of N–Na is 2.59 Å. After four Na atoms are inserted in the crystal unit cell, the valence of Fe changes from Fe^{3+} to Fe^{2+}, and magnetism of the material is quenched (the local magnetic moment of Fe becomes zero). We further calculate the phonon dispersion of the system with one Na inserted and the results are shown in Fig. 2(b). We can see that there is no imaginary frequency, indicating that the configuration with Na insertion at the center of the quadrate is stable. However, the diffusion barrier of Na from the center of the quadrate to the void of the cubic unit is small (~0.36 eV). Thus the inserted Na should easily diffuse into the void of the cubic unit at room temperature. It may be the reason that the guest Na seems to be located at the center of the small cubic structural unit experimentally at room temperature.

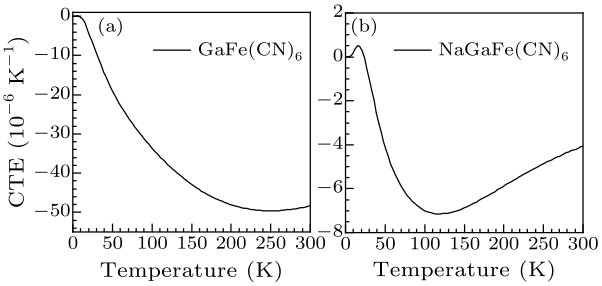

Fig. 4. (a) Calculated CTE of $GaFe(CN)_6$, and (b) CTE of one Na inserted in $GaFe(CN)_6$.

The main feature of the phonon dispersion of the Na-inserted system is similar to that of the pristine one. The vibration modes involving Na are distributed in the lowest band. To better understand the effect of Na insertion on the thermal expansion of the system, we calculate the Grüneisen parameters of the one Na-inserted system as shown in Fig. 5(a) (four Na atoms can be inserted in a unit cell at most). The

mode Grüneisen parameter at frequency 39 cm^{-1} is 12, which is positive and caused mainly by the vibration of the inserted Na. The corresponding vibration of atoms is shown in Fig. 5(b). The mode makes the system exhibit positive thermal expansion at very low temperature (see the calculated CTE shown in Fig. 4(b)). With the increasing temperature, the modes with negative Grüneisen parameters are excited and dominated. The system then exhibits NTE with negative CTE. In Figs. 5(c) and 5(d), the two vibration modes at frequencies of 72 cm^{-1} and 73 cm^{-1} are given, where cyanide groups vibrate along transverse directions with the negative Grüneisen parameters. The detailed analysis shows that the number of transverse vibration modes is decreased due to the Na insertion, and the more Na is inserted, the greater the decrease in the number of transverse modes. Thus the NTE of the system becomes less pronounced and even positive when more and more Na atoms are inserted because of the prohibition of more transverse vibration modes of the cyanide group (CN group).[35]

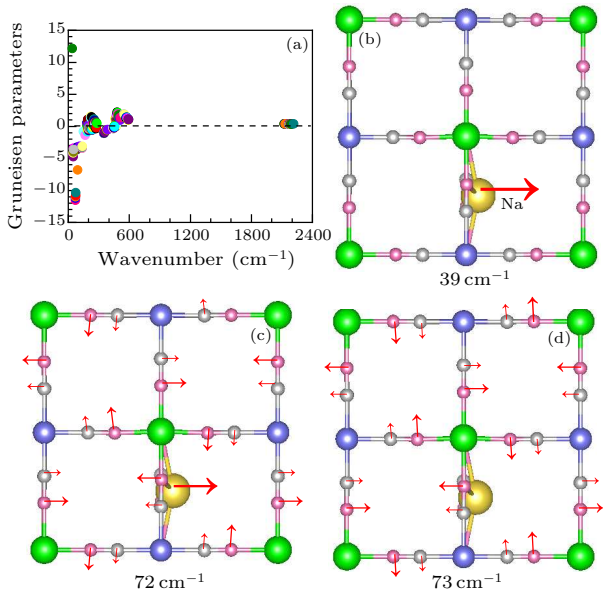

Fig. 5. (a) Calculated Grüneisen parameters of one Na inserted in $GaFe(CN)_6$. (b), (c) and (d) The vibration modes at the low frequencies of 39 cm^{-1}, 72 cm^{-1} and 73 cm^{-1}, respectively.

The volume CTE of the one Na-inserted system $GaFe(CN)_6$ is calculated in the temperature range 0–300 K as shown in Fig. 4(b). Because the inserted Na is easily diffused from the binding site to the void of the cubic cell at high temperatures, the highest temperature is taken as 300 K for the CTE calculations to avoid the occurrence of this situation. The average volume CTE is $\sim -6\times10^{-6}\,K^{-1}$ in this temperature range. Comparing the volume CTEs of the two systems with and without Na insertion, it can be found that the insertion of Na can effectively reduce the negative CTE of the system. However, we notice that the difference of our calculated volume CTEs for the systems with and without one Na insertion is larger than that found in the experimental data.[35] The reasons are probably due to the pronounced anharmonic effect of the systems as well as the GGA and QHA approximations used in our calculations.

In summary, $GaFe(CN)_6$ exhibits NTE due to the transverse vibration modes of cyanide groups. When guest Na is inserted in the framework of the material, it prefers to locate at the center of quadrates of the cubic unit and binds to the four N atoms nearby. However, the inserted Na is easily diffused into the void of the cubic unit at high temperatures. After Na insertion, the transverse vibration modes of cyanide groups are hindered, and the NTE of the system is weakened due to the damping of the lateral vibrations of the cyanide groups. By adjusting the inserted Na concentration, the CTE of the system can be tuned from negative to positive. Our calculations clarify the mechanisms of the NTE and the damping effect of the inserted Na on the NTE of the framework material.

References

[1] Mary T A et al 1996 *Science* **272** 90
[2] Chen J et al 2010 *Physics* **691** 698 (in Chinese)
[3] Mohn P 1999 *Nature* **400** 18
[4] Attfield J P 2011 *Nature* **480** 465
[5] Dove M T and Fang H 2016 *Rep. Prog. Phys.* **79** 066503
[6] Dubbeldam D et al 2007 *Angew. Chem. Int. Ed.* **46** 4496
[7] Salvador J R et al 2003 *Nature* **425** 702
[8] Arvanitidis J et al 2003 *Nature* **425** 599
[9] Takenaka K and Takagi H 2005 *Appl. Phys. Lett.* **87** 261902
[10] Hao Y et al 2001 *Appl. Phys. Lett.* **78** 3277
[11] Li W H et al 2002 *Phys. Rev. Lett.* **89** 135504
[12] Zakharchenko K V et al 2009 *Phys. Rev. Lett.* **102** 046808
[13] Evans J S O et al 1997 *J. Solid State Chem.* **133** 580
[14] Mary T A and Sleight A W 1999 *J. Mater. Res.* **14** 912
[15] Mittal R and Chaplot S L 1999 *Phys. Rev. B* **60** 7234
[16] Tallentire S E, Child F, Fall I et al 2013 *J. Am. Chem. Soc.* **135** 12849
[17] Greve B K et al 2010 *J. Am. Chem. Soc.* **132** 15496
[18] Chen J et al 2017 *Nat. Commun.* **8** 14441
[19] Hu L et al 2016 *J. Am. Chem. Soc.* **138** 8320
[20] Goodwin A L and Kepert C J 2005 *Phys. Rev. B* **71** 140301
[21] Chapman K W et al 2006 *J. Am. Chem. Soc.* **128** 7009
[22] Margadonna S et al 2004 *J. Am. Chem. Soc.* **126** 15390
[23] Goodwin A L et al 2005 *J. Am. Chem. Soc.* **127** 17980
[24] Goodwin A L et al 2008 *Science* **319** 794
[25] Duyker S G et al 2013 *Angew. Chem.* **125** 5374
[26] Gao Q L et al 2017 *Angew. Chem. Int. Ed.* **56** 9023
[27] Han S S and Goddard W A 2007 *J. Phys. Chem. C* **111** 15185
[28] Grobler I et al 2013 *J. Am. Chem. Soc.* **135** 6411
[29] Zhou H L et al 2015 *Nat. Commun.* **6** 6917
[30] Ohkoshi S et al 2007 *Angew. Chem.* **119** 3302
[31] Kaye S S and Long J R 2005 *J. Am. Chem. Soc.* **127** 6506
[32] Gao Q L et al 2018 *Inorg. Chem. Front.* **5** 438
[33] Patra C R 2016 *Theranostics. Nanomed.* **11** 569
[34] Gao Q L et al 2018 *Inorg. Chem.* **57** 10918
[35] Gao Q L et al 2018 *Inorg. Chem.* **57** 14027
[36] Kresse G and Furthmüller J 1996 *Phys. Rev. B* **54** 11169
[37] Kresse G 1999 *Phys. Rev. B* **59** 1758
[38] John K B et al 1996 *Phys. Rev. Lett.* **77** 3865
[39] Togo A et al 2008 *Phys. Rev. B* **78** 134106
[40] Wang L et al 2014 *Mater. Chem. Phys.* **148** 214
[41] Wang Z et al 2013 *J. Appl. Phys.* **114** 063508
[42] Chang D et al 2016 *Phys. Chem. Chem. Phys.* **18** 14503
[43] Chang D et al 2017 *Phys. Rev. B* **95** 104101
[44] Chang D et al 2017 *Phys. Chem. Chem. Phys.* **19** 2067
[45] Souvatzis P and Eriksson O 2008 *Phys. Rev. B* **77** 024110